Postharvest Biology and Technology 67 (2012) 96–101

Contents lists available at SciVerse ScienceDirect

Postharvest Biology and Technology

journal homepage: www.elsevier.com/locate/postharvbio

# Black heart characterization and detection in pomegranate using NMR relaxometry and MR imaging

Lu Zhang [a], Michael J. McCarthy [a,b,*]

[a] Department of Food Science and Technology, University of California, One Shields Avenue, Davis, CA 95616, United States
[b] Department of Biological and Agricultural Engineering, University of California, One Shields Avenue, Davis, CA 95616, United States

ARTICLE INFO

*Article history:*
Received 4 August 2011
Accepted 31 December 2011

*Keywords:*
Pomegranate
Black heart
Magnetic resonance imaging
$T_2$ relaxation time

ABSTRACT

In pomegranate, black heart disease develops inside the fruit without affecting the rind. Visual inspection is not effective for identification of black heart in pomegranate fruit because of the lack of external symptoms. It has been shown that the water proton $T_2$ relaxation time is sensitive to cell compartmentalization. Proton NMR relaxometry was used to investigate the water $T_2$ relaxation distribution in infected and healthy pomegranate arils, and to obtain information that indicates tissue damage. Multi-exponential inversion of the $T_2$ data of healthy arils gave three relaxation peaks, which correspond to different water compartments in tissue. In infected arils, the three relaxation components shifted to lower relaxation time and a new fast relaxation component appeared indicating there was water redistribution among cell compartments caused by the infection. The change in cell membrane integrity in arils was also investigated with the aid of paramagnetic ions. $T_2$-weighted fast spin echo images were acquired for healthy and pomegranates with black heart. Histogram features of images, including mean, median, mode, standard deviation, skewness, and kurtosis, were examined using partial least square discriminant analysis (PLS-DA). The PLS-DA model based on histogram features of MR image showed 92% accuracy in detecting the presence of black heart in pomegranate fruit. The significant change in $T_2$ relaxation distribution in arils after infection proved that $T_2$ relaxation time is a good indicator of black heart in pomegranate. The $T_2$ based MR imaging showed its potential as a nondestructive technique for black heart detection in pomegranate.



## 1. Introduction

Black heart, also know as "heart rot", is a major pomegranate disease impacting production in California. Although black heart is always recognized as a postharvest quality problem, the infection begins in the orchard. *Alternaria* spp. or *Aspergillus* spp. enters the fruit during bloom and early fruit set, grows and spreads within the fruit as the fruit develops. After penetration into the host tissue, fungal pathogens attack the fruit by producing cuticle and cell wall degrading enzymes, toxins, and detoxifying resistance compounds in the host. In response to the fungal infection, the hosts produce antimicrobial compounds, such as phytoalexins and active oxygen species, reinforce the physical barrier, or initiate localized cell death to prevent the pathogen from spreading. The pathogen–host interaction may induce a number of alterations in the physiological and biochemical processes or in the host tissue constituents (Barkai-Golan, 2001). However, the fungi cause decay of arils ranging from sections of the pomegranate fruit to all the arils within the rind without external symptoms except for slightly abnormal skin color or soft spot (Seeram et al., 2006). The lack of obvious external symptoms makes black heart identification a challenge for sorters in the packinghouse or processing line. A fast non-destructive technique capable of probing the interior of pomegranate and detecting the infection is needed for fruit used for the fresh market and processing. If the alteration in cell structure and tissue constituents in arils could be identified after fungal infection, it would be possible to detect the black heart in pomegranate caused by *Alternaria* spp. and *Aspergillus* spp.

Nuclear Magnetic Resonance (NMR) water proton relaxometry has been used to study the physiological changes in plant tissue induced by different treatments or natural factors. The proton spin–lattice ($T_1$) relaxation time and spin–spin ($T_2$) relaxation time are related to the water content, physical properties of water, and interaction of water with macromolecules (Van As, 1992). In compartmentalized systems, e.g., plant cell, proton relaxation time is often a multiexponential process, indicating the presence of multiple water compartments with different relaxation times in a plant tissue (Belton and Ratcliffe, 1985). The multiexponential nature

* Corresponding author at: Department of Food Science and Technology, University of California, Davis, One Shields Avenue, Davis, CA 95616, United States.
Tel.: +1 530 752 8921; fax: +1 530 752 4759.
*E-mail address:* mjmccarthy@ucdavis.edu (M.J. McCarthy).

0925-5214/$ – see front matter © 2012 Elsevier B.V. All rights reserved.
doi:10.1016/j.postharvbio.2011.12.018

of the water proton relaxation in a plant cell makes it a useful tool to study the cellular compartmentalization and distribution of water in plant tissue. $T_2$ relaxometry was used to explore the effect of high pressure, freezing, drying, or ripening on the physiological change at sub-cellular level in apple, tomato, strawberry, banana, and onion (Ersus et al., 2010; Hills and Remigereau, 1997; Marigheto et al., 2004, 2009; Raffo et al., 2005). Generally, three or four proton relaxation components have been identified in fruit and vegetable tissues. The first three have been assigned to the vacuole, the cytoplasm, and the cell wall. The additional peak was considered to be associated with extracellular water or starch or non-exchangeable macromolecular protons in different fruit tissues (Musse et al., 2009; Raffo et al., 2005; Sibgatullin et al., 2007). In tomato pericarp tissue, the identity of the fourth peak was determined experimentally by Musse et al. (2010), and they confirmed that the fourth peak was corresponded to the water protons instead of macromolecule. A reliable assignment of relaxation peaks to sub-cellular compartments, especially the minor components, is difficult to obtain. Among all the effort made to clear up the uncertainty in relaxation components assignment, a paramagnetic ion was frequently used as a probe to detect the water distribution in plant cells or animal cells. Paramagnetic ions or complexes like $Mn^{2+}$ enhance the relaxation rate of water when it is in contact with water proton, thus the $T_2$ relaxation time of each compartment in fruit tissue can be affected as the paramagnetic $Mn^{2+}$ penegrate successively into extracellular space, cytoplasm, and vacuole (Snaar and Van As, 1992). The paramagnetic ion tracer was used by Snaar and Van As (1992) to investigate the water compartments and permeability of membranes in plant cells. Only a few studies were conducted using $T_2$ relaxometry to investigate the effect of fungal infection on plant tissue. Van As (1992) observed change in the dehydration pattern of water compartments in wheat plant leaf after fungal infection using $T_2$ relaxometry. Attempts have also been made to study the fungal infection in fruit and vegetables using magnetic resonance imaging (MRI). MRI enables the acquisition of spatial resolved images in which water proton relaxation time information is encoded. The progress of infection following *Botrytis cinerea* inoculation was traced in raspberry and strawberry by MRI (Goodman et al., 1992; Maas and Line, 1995). Potato tuber was found to respond differently to various fungal pathogens, and this is discernible in MR images (Snijder et al., 1996).

The objectives of this study were to determine the effect of the physiological changes induced by *Alternaria* spp. or *Aspergillus* spp. on the $T_2$ relaxation behavior of pomegranate, and to determine whether it is possible to use MR imaging as a non-destructive method of detecting black heart in pomegranate fruit.

## 2. Materials and methods

### 2.1. Materials

Pomegranates of variety "Wonderful" were supplied by POM Wonderful (Del Rey, CA), which were harvested at the maturity of ripe stage from the orchard. The fruit were pre-screened to ensure large quantity of black heart fruit and avoid other defects in the collected samples.

### 2.2. NMR relaxometry

#### 2.2.1. $T_2$ relaxation measurement

Arils are the only affected area in the pomegranates with black heart. Arils were separated manually from the fruit for relaxometry study. Five samples of normal and infected arils were obtained from different healthy and black heart fruit. Each sample contained approximately 20–25 arils (~10 g). NMR relaxometry measurements were performed on a 1 T NMR spectrometer (Aspect AI, Industrial Area Hevel Modi'in, Shoham, Israel). $T_2$ was measured using a Carr–Purcell–Meiboom–Gill sequence with echo time of 1 ms and 8000 echoes were recorded. The $T_2$ relaxation decay curve was transformed into a continuous spectrum of $T_2$ relaxation components by Non-negative Least Square Algorithm using Prospa V2.2.17 (Magritek, New Zealand).

#### 2.2.2. Paramagnetic ion tracer experiment

Normal and infected arils with a sample size of about 10 g were immersed in 50 mM $MnCl_2$ solution. The $T_2$ relaxation time of each sample was recorded periodically for 6 h. Arils were blotted dry before they were interrogated. $T_2$ spectrum inversion was performed on the raw data to monitor the change in each relaxation component. Four replicates were obtained for normal and infected arils, respectively.

### 2.3. MR imaging

MRI data were acquired on the same 1 T spectrometer as described in Section 2.2.1 with a 60 × 90 mm elliptical RF coil. The coil can accept fruit with a height less than 56 mm and an equatorial diameter less than 85 mm. Samples were trimmed by removing primarily the rind to accommodate to the size of the coil, placed on a plastic sample holder and then manually centered to obtain an image of the equatorial slice of each fruit. MR images were generated using a Fast Spin Echo (FSE) sequence with effective echo time ($TE_{eff}$) of 500 ms, repetition time (TR) of 8000 ms, slice thickness of 5 mm, and Field of View (FOV) of 95 mm × 95 mm. In Fast Spin Echo images, the signal intensity is given by (Bernstein et al., 2004):

$$S = S_0 e^{-TE_{eff}/T_2} \quad (1)$$

where $S_0$ is the net magnetization and $T_2$ is the spin–spin relaxation time. The image contrast is predominantly determined by the central area in $k$-space. The $TE_{eff}$ is the time when the central $k$-space data are acquired, so the signal intensity in FSE image is primarily a function of $TE_{eff}$. The long $TE_{eff}$ used in imaging makes the FSE images $T_2$ weighted. After imaging, samples were sliced to examine the fruit interior for black heart. MR images of 177 pomegranates were acquired, 139 fruit containing black heart.

### 2.4. Image analysis

A square region of interest (ROI) was defined in the MR image (Fig. 1). Quantitative analysis of the ROI was achieved by extracting statistical features of the signal intensity, including mean, median, mode, standard deviation, skewness, kurtosis, and coefficient of variation.

Partial least square-discriminant analysis (PLS-DA) was carried out on the statistical features of the signal intensity in ROI of MR images to develop a classification model. In the PLS-DA model, the 7 features of signal intensity were used as independent variables $X$. The class identity of each sample, i.e., black heart or healthy, was used as the response variable $Y$. The black heart class was designated as the positive response (1) and negative response (0) was assigned to healthy class. The model was developed using Matlab 2010a (The Mathworks, Natick, MA) and PLS_toolbox (Eigenvector Research Inc., Wenatchee, WA). In order to evaluate the performance of the model, a 3-fold cross-validation was performed by randomly partition the data into 3 subgroups. Two groups were used as training data to build a model, and the remaining group was applied to the developed model as the validation data for testing the model. The process was repeated for 3 times, with each of the subgroups used once as the validation data. The 3-fold random cross-validation was iterated for 7 times.

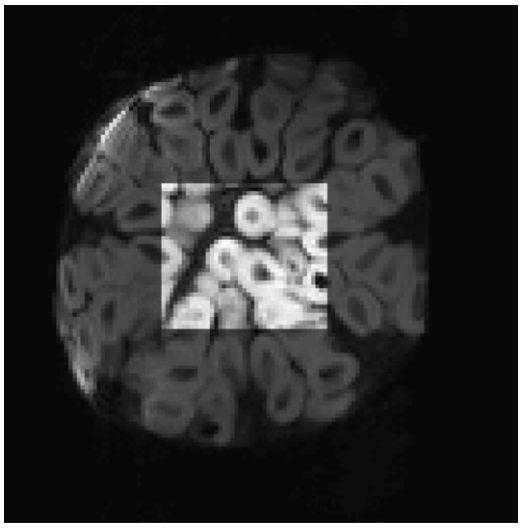

**Fig. 1.** ROI (highlighted) of a pomegranate MR image.

## 3. Results and discussion

### 3.1. NMR relaxometry

#### 3.1.1. $T_2$ relaxation time

Multiexponential inversion of the $T_2$ relaxation data decomposes the data into several components with different relaxation times. In healthy arils, three peaks were observed in the $T_2$ spectrum (Fig. 2a). The multiexponential relaxation behavior in plant cells originates from the multicompartment nature of the plant cellular tissue (Hills and Clark, 2003). Each relaxation component is associated with a water/proton compartment in a plant cell. The peak with the shortest $T_2$ relaxation time (peak 1) may be attributed to the water in the cell wall. The cell wall water is present in very small pores and strong water-binding sites, held by matrix and molecular force (Black, 2002). Short $T_2$ relaxation time, induced by the restricted water movement and fast proton exchange between water and macromolecules, should be expected for the water in cell wall. Peak 2 was assigned to cytoplasm. In cytoplasm, some of the water is hydrogen-bonded to side chains of the proteins forming the framework of the protoplasm (Kramer, 1983). The water in cytoplasm would have an intermediate $T_2$ value given the nature of cytosol (Raffo et al., 2005). In plant cells, 50–80% or more of the water occurs in the vacuoles (Kramer, 1983), thus peak 3 with the longest relaxation time and highest signal intensity should be associated with the water in the vacuole. In the infected arils, four components were identified in the $T_2$ spectrum (Fig. 2b). As explained below, the peaks shifted to the left (shorter relaxation times) and a new peak appeared between what were previously peaks 1 and peak 2, indicating the occurrence of a new water compartment. According to the $T_2$ distribution in apple tissue (Sibgatullin et al., 2007), the new component may be attributed to extracellular water. Following penetration into fruit tissue, fungus produces pectolytic and cellulolytic enzymes. The enzymes are capable of decomposing the cell wall and the tight link between cells – middle laminar, causing tissue disintegration and cell separation. The enzymatic hydrolysis of cell wall and middle laminar enhances the permeability of the cell membrane of infected tissue and facilitate the diffusion of nutrients from intracellular space to intercellular space (Rivka, 2001). In addition, some fungal invaders secrete phytotoxins, inhibiting host cell function. The host specific toxins produced by different *Alternaria* spp. affect plasma membrane and cause permeabilization (Thomma, 2003). As a result, leakage of nutrients to the intercellular space leads to the extracellular water in infected tissue.

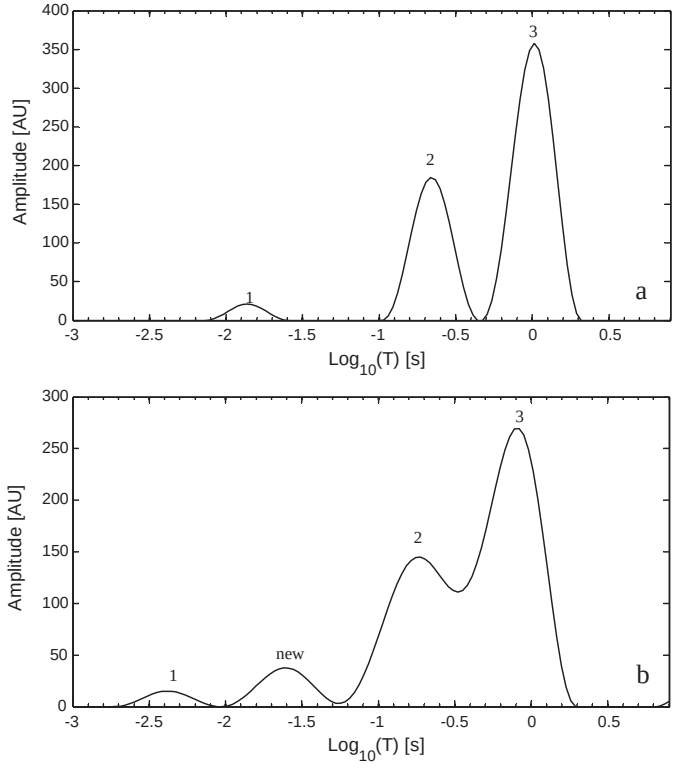


**Fig. 2.** $T_2$ relaxation spectrum of arils from (a) a healthy pomegranate and (b) a pomegranate with black heart.

**Table 1**
$T_2$ relaxation time and relative signal intensity of the relaxation components in healthy and infected arils.*

| | Peak 1 | | Peak new | | Peak 2 | | Peak 3 | |
|---|---|---|---|---|---|---|---|---|
| | $T_2$ (s) | M% | $T_2$ (s) | M% | $T_2$ (s) | M% | $T_2$ (s) | M% |
| Healthy | 0.011[a] | 3.93[a] | – | – | 0.204[a] | 26.9[a] | 1.002[a] | 69.2[a] |
| Infected | 0.007[b] | 4.71[a] | 0.033 | 9.45 | 0.166[b] | 37.7[b] | 0.736[b] | 48.2[b] |

* Values with different letters in the same column are significantly different at $P = 0.05$.

The well defined peak 2 and peak 3 in the relaxation spectrum of healthy arils partially merged together in the $T_2$ spectrum of infected arils. Diffusion of water between the sub-cellular compartments averages the water proton magnetization to an extent depending on geometry and membrane permeability (Hills and Duce, 1990). The less separated peaks in spectrum of infected arils is a result of greater diffusive averaging effect, resulting from an increase in the permeability and/or loss of integrity of the tonoplast, the barrier between vacuole and cytoplasm.

Quantitative analysis of the $T_2$ distributions is summarized in Table 1. $T_2$ values of all of the three components showed significant decrease. Such decrease is consistent with the observation of small $T_2$ values in *Phytophthora infestans* infected potato tubers, which was attributed to the increase in the level of free radicals in tissue as measured by EPR (Snijder et al., 1996). The paramagnetic free radical facilitates the water proton relaxation process, decreasing the $T_2$ relaxation time. In addition, the change in $T_2$ value may be explained by the loss of moisture and degradation of macromolecules, e.g., polysaccharides and proteins, from the fungus infection.

Water redistribution was observed as indicated by the change in the relative signal intensity (M%) of each cell components. The signal intensity of peak 3 (vacuole) decreased from 69.2% in healthy

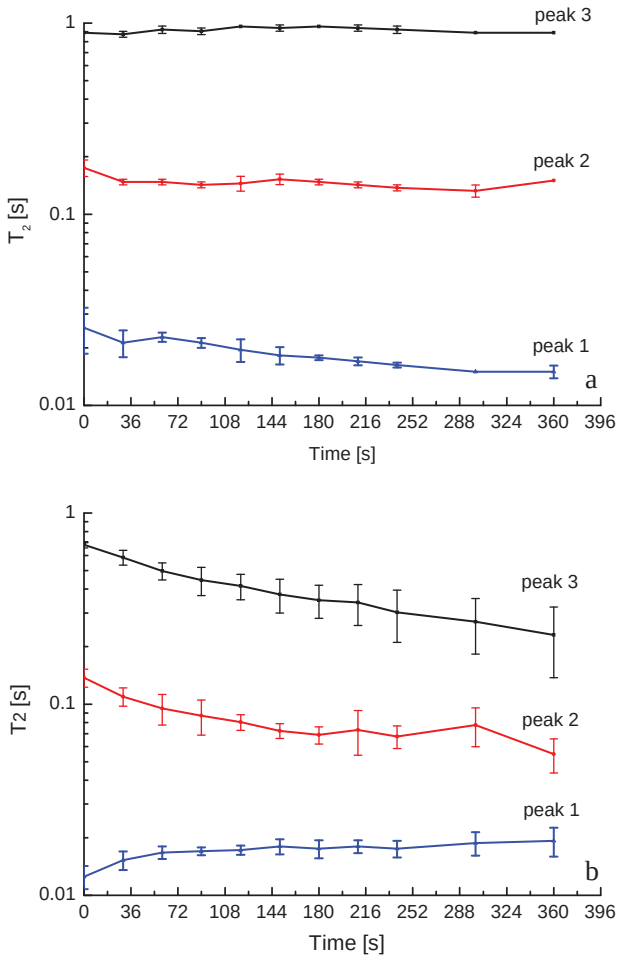


**Fig. 3.** The effect of $Mn^{2+}$ ions on the $T_2$ relaxation time of water in (a) healthy pomegranate arils (b) infected pomegranate arils as a function of immersion time.

arils to 48.2% in infected arils, whereas the intensity of peak 2 (cytoplasm) increased from 26.9% to 37.7%. The rise in the signal intensity of peak 1 (cell wall) was not significant. The new peak (extracellular water) accounted for 9.45% of the total signal intensity. The variation trend in the signal intensity reflects that water transferred out from the vacuole to the cytoplasm and the extracellular space. Cell membranes, tonoplast and plasma membrane, are the boundary layers that regulates the water and solute movement through the regions they separate in plant cells. In infected arils, the compromised integrity of the cell membranes is the main reason for the water redistribution.

### 3.1.2. Paramagnetic ion tracer experiment

To obtain more information on the cell structure and integrity in the healthy and infected arils, arils were immersed in a solution doped with low dose of $MnCl_2$, a paramagnetic tracer capable of diffusing into tissue. In healthy arils, The $T_2$ value of peak 3 (vacuole) stayed almost constant over the whole period of soaking (Fig. 3a). The shortest $T_2$ component demonstrated significant decrease in $T_2$ during the 6 h of soaking time; while a small decrease in the $T_2$ value of peak 2 (cytoplasm) was observed. Low dose of paramagnetic agents enhance $T_2$ relaxation through electron–nuclear dipolar interactions. These interactions take place only when the water molecules enter within the immediate hydration sphere of the paramagnetic ion (Donahue et al., 1997). In cells, barriers exits between compartments restricting the diffusion of the paramagnetic agent through compartments and limiting the $T_2$ reducing effect of the agent. $Mn^{2+}$ ions are able to penetrate into the tissue via extracellular space, and successively into the cytoplasm, and vacuole through membranes (Snaar and Van As, 1992). Therefore, evident decrease in $T_2$ value was first observed in peak 1 (cell wall). Following the movement of $Mn^{2+}$ ion into the cell wall, small amount of $Mn^{2+}$ ion penetrated through the plasma membrane and entered the cytoplasm, as indicated by the small decrease in the $T_2$ of peak 2. Although $Mn^{2+}$ is a membrane permeable ion, the immersion time 6 hr is not long enough for the ion to diffuse through the plasma membranes. Thus, peak 3 (vacuole) did not demonstrate any change in $T_2$ relaxation time. The sequential order and the extent of the change in $T_2$ value of each relaxation component provided more evidence in support of the peak assignment.

In infected arils, the $T_2$ relaxation time of peak 2 (cytoplasm) and peak 3 (vacuole) gradually declined starting from 30 min (Fig. 3b). A slight increase in $T_2$ was observed in peak 1 (cell wall). The divergence in the variation of $T_2$ value of cell compartments in healthy and infected arils is indicative of the change in cell integrity after infection. The penetration process of $Mn^{2+}$ ions into cytoplasm and vacuole was markedly faster than in healthy arils. This penetration, just like the changes in the signal intensity of distribution components, indicates the cell membrane in arils lost their integrity after infection.

Besides the three compartments mention above, a new relaxation component was detected in infected arils. This component in infected samples disappeared completely after 60 min. The disappearance of the component may be due to the drastic reduction in its $T_2$, so that the peak cannot be detected within the measured time frame. This fraction of the water is not restrained by the cell wall and should be easily accessed by and interact with the $Mn^{2+}$ ions. This also provides more evidence that this component of relaxation is associated with extracellular water.

## 3.2. MR imaging

### 3.2.1. Visualization of black heart

Fig. 4 shows images of a healthy pomegranate and a pomegranate with black heart. Because of the large difference in the structure of pomegranate tissues like arils and rind, their corresponding area in the MR image possess a distinct signal intensity. Arils were clearly visible in the MR images, while the rind was dim. In healthy pomegranates, all arils within the rind can be recognized in the image (Fig. 4a). In the black heart fruit, there was a reduction of signal intensity for portions of the aril. Some void areas were observed in the arils region of severely infected fruit (Fig. 4b). In the portions of pomegranate with black heart, there was a significant loss in signal compared to neighboring regions. The long $TE_{eff}$ determines that the contrast in the image is $T_2$ weighted. NMR relaxometry results showed that the $T_2$ relaxation time in the black heart tissue was significantly lower than in the healthy tissue. The short $T_2$ relaxation time accounts for the low signal intensity of the black heart area in the pomegranate. Moreover, the severely damaged arils demonstrated extensive water loss, which also contributes to the lower signal intensity.

### 3.2.2. PLS-DA model for black heart detection

The use of discriminant analysis for classification of pomegranate based on the presence of black heart requires quantitative input data rather than images. In order to extract quantitative information from MR images, statistical features of pomegranate images were calculated to characterize the overall signal intensity change and variance in the images.

The PLS-DA model was developed on the basis of 7 MR image features and class membership of fruit with or without black heart. Random subset cross-validation helps to optimize and validate

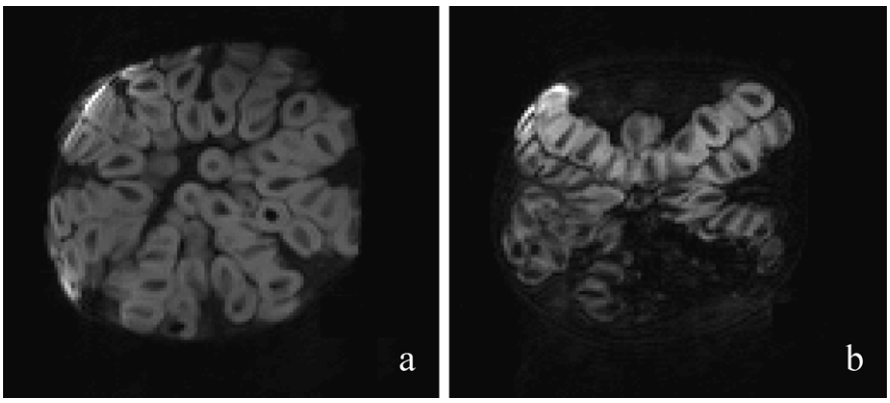


**Fig. 4.** Example MR images of (a) a healthy pomegranate and (b) a pomegranate with black heart.

an effective multivariate model. A PLS-DA model with the first 4 latent variables was chosen as the root mean square error of cross-validation (RMSECV) leveling off at 4 latent variables. The model captured 93% of the variance in independent variables (image features) and 66% of the variance in the response variable (pomegranate class). The classification error rate of the calculated model is 5%, meaning 5% of the samples were misclassified. The cross-validated model had a classification error of 8%, a 3% loss in the accuracy compared to the calculated model. The small change in the classification error rate after performing cross-validation demonstrated that the performance of this model won't degrade when applied to a new dataset. Fig. 5 depicts the model performance of the cross-validated PLS-DA model in predicting the presence of black heart in samples. The model calculated scores, which are projection of the samples in the space constructed by the 4 latent variables, for each of the 177 samples. The score, *y* axis in Fig. 5, is a prediction for the membership of each sample. A threshold for binary classification was calculated using a Baysian method, shown as the dashed line in Fig. 5. Samples with a score greater than the threshold are classified as pomegranates with black heart, and points below the threshold line are the healthy samples. Most of the black heart fruit stayed above the threshold line, but several black heart samples failed the criteria. The sensitivity, true positive (black heart) rate, was 93%, whereas the specificity, true negative (healthy) rate was 91%. Although the fruit was trimmed before imaging, the black heart related portion of the pomegranate was not impacted by the trimming. The incidence of black heart is random within the arils, so the location of the infection could be anywhere within the fruit. The images acquired in this study were central slices of fruit with 5 mm thickness, which is a possible cause of misclassification if the black heart was not contained in the slice. A classification rate greater than 92% can be expected by increasing the thickness of the image slice.

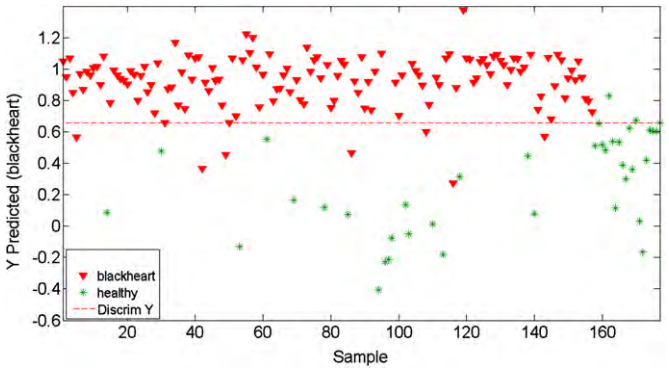


**Fig. 5.** PLS-DA model prediction for presence of black heart in pomegranates.

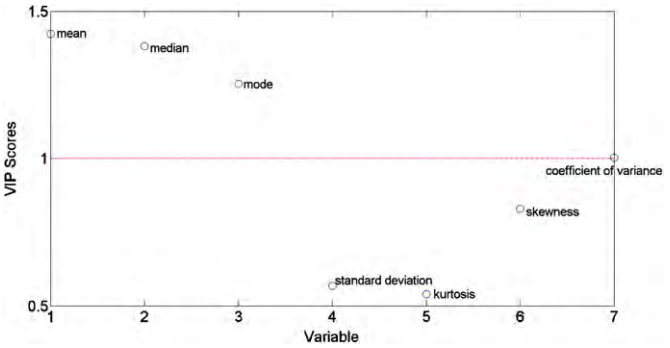


**Fig. 6.** VIP score plot of independent variables in the PLS-DA model for identifying black heart.

Variable importance in projection (VIP) scores for each independent variable were calculated to evaluate their relative importance in the black heart PLS-DA prediction model (Fig. 6). Mean, median, mode, coefficient of variation of the signal intensity had VIP scores greater than one, implying they were most influential for the model. These variables are the image features that best explain the difference between MR images of healthy and black heart pomegranates. The black heart region in pomegranate reduced the signal intensity and created abnormal area distinct from surrounding tissue in the image. The mean, median, and mode reflected the general drop in the signal intensity. One of the best variables to use for detection of black heart is the coefficient of variation, which is the standard deviation normalized by dividing it by the mean, so it is able to capture the occurrence of black heart.

## 4. Conclusion

NMR relaxometry measurement gave an indication of the extent and type of disruption of the pomegranate tissue at the sub-cellular level that is caused by black heart disease. The infection induced alteration in the microstructure in arils and caused significant change in the $T_2$ relaxation spectrum. Important information on water redistribution in aril tissue after infection was obtained using NMR relaxometry. The paramagnetic ion study further supported the physiological changes observed in relaxation measurement, such as the change in the integrity of the cell membrane.

$T_2$-weighted MR image made it possible to visualize the black heart in the fruit non-destructively. Black heart region in the pomegranate can be easily recognized in the MR image.

Using the mean, median, mode, standard deviation, skewness, kurtosis, and coefficient of variation of the signal intensities in the image, the PLS-DA model was able to correctly identify the presence of black heart in pomegranate fruit with an accuracy of over 92%. It

should be possible to increase the accuracy by using a slice thicker than the 5 mm thickness used in this study. Therefore, the results of this study indicate that MR imaging has potential as a nondestructive technique for detection of blackheart in pomegranate.

## Acknowledgements

This work was partially supported by POM Wonderful LLC and by National Research Initiative Award 2007-02632 from the USDA National Institute of Food and Agriculture.

## References

Barkai-Golan, R., 2001. Postharvest Diseases of Fruits and Vegetables: Development and Control. Elsevier, New York.
Belton, P.S., Ratcliffe, R.G., 1985. NMR and compartmentation in biological tissues. Progress in Nuclear Magnetic Resonance Spectroscopy 17, 241–279.
Bernstein, M., King, K., Zhou, X., 2004. Handbook of MRI Pulse Sequences. Academic Press.
Black, M.P.H.W., 2002. Desiccation and Survival in Plants: Drying without Dying. CABI, Wallingford, Oxon, UK.
Donahue, K.M., Weisskoff, R.M., Burstein, D., 1997. Water diffusion and exchange as they influence contrast enhancement. Journal of Magnetic Resonance Imaging 7, 102–110.
Ersus, S., Oztop, M.H., McCarthy, M.J., Barrett, D.M., 2010. Disintegration efficiency of pulsed electric field induced effects on onion (*Allium cepa* L.) tissues as a function of pulse protocol and determination of cell integrity by $^{1}$H NMR relaxometry. Journal of Food Science 75, E444–E452.
Goodman, B.A., Williamson, B., Chudek, J.A., 1992. Non-invasive observation of the development of fungal infection in fruit. Protoplasma 166, 107–109.
Hills, B.P., Clark, C.J., 2003. Quality assessment of horticultural products by NMR. Annual Reports on NMR Spectroscopy 50, 76.
Hills, B.P., Duce, S.L., 1990. The influence of chemical and diffusive exchange on water proton transverse relaxation in plant tissues. Magnetic Resonance Imaging 8, 321–331.
Hills, B.P., Remigereau, B., 1997. NMR studies of changes in subcellular water compartmentation in parenchyma apple tissue during drying and freezing. International Journal of Food Science & Technology 32, 51–61.
Kramer, P.J., 1983. Water Relations of Plants. Academic Press, New York, NY.
Maas, J.L., Line, M.J., 1995. Nuclear magnetic resonance (NMR) inversion recovery spin echo microimaging of fungus infections in strawberry fruit. Acta Horticulture 398, 241–248.
Marigheto, N., Moates, G., Furfaro, M., Waldron, K., Hills, B., 2009. Characterisation of ripening and pressure-induced changes in tomato pericarp using NMR relaxometry. Applied Magnetic Resonance 36, 35–47.
Marigheto, N., Vial, A., Wright, K., Hills, B., 2004. A combined NMR and microstructural study of the effect of high-pressure processing on strawberries. Applied Magnetic Resonance 26, 521–531.
Musse, M., Cambert, M., Mariette, F., 2010. NMR study of water distribution inside tomato cells: effects of water stress. Applied Magnetic Resonance 38, 455–469.
Musse, M., Quellec, S., Cambert, M., Devaux, M.F., Lahaye, M., Mariette, F., 2009. Monitoring the postharvest ripening of tomato fruit using quantitative MRI and NMR relaxometry. Postharvest Biology and Technology 53, 22–35.
Raffo, A., Gianferri, R., Barbieri, R., Brosio, E., 2005. Ripening of banana fruit monitored by water relaxation and diffusion $^{1}$H NMR measurements. Food Chemistry 89, 149–158.
Rivka, B.-G., 2001. Chapter 5 – Attack Mechanisms of the Pathogen, Postharvest Diseases of Fruits and Vegetables. Elsevier, Amsterdam, pp. 54–65.
Seeram, N.P., Schulman, R.N., Heber, D., 2006. Pomegranates: Ancient Roots to Modern Medicine. CRC Press, Boca Raton, London & New York.
Sibgatullin, T., de Jager, P., Vergeldt, F., Gerkema, E., Anisimov, A., Van As, H., 2007. Combined analysis of diffusion and relaxation behavior of water in apple parenchyma cells. Biophysics 52, 196–203.
Snaar, J.E.M., Van As, H., 1992. Probing water compartments and membrane permeability in plant cells by $^{1}$H NMR relaxation measurements. Biophysical Journal 63, 1654–1658.
Snijder, A.J., Wastie, R.L., Glidewell, S.M., Goodman, B.A., 1996. Free radicals and other paramagnetic ions in interactions between fungal pathogens and potato tubers. Biochemical Society Transactions 24, 442–446.
Thomma, B.P.H.J., 2003. *Alternaria* spp.: from general saprophyte to specific parasite. Molecular Plant Pathology 4, 225–236.
Van As, H., 1992. NMR in horticulture: in situ plant water balance studies with NMR. Acta Horticulture 304, 103–112.